Int J Thermophys (2008) 29:678–692
DOI 10.1007/s10765-007-0315-7

Thermal Conductivity of High-Temperature Multicomponent Materials with Phase Change

K. S. do Couto Aktay · R. Tamme · H. Müller-Steinhagen

Published online: 7 December 2007

Abstract This work focuses on the investigation of the effective thermal conductivity (λ_{eff}) of heterogeneous materials consisting of a phase change material (PCM) and expanded graphite (EG). These composites may be employed in latent heat storage systems, where a PCM stores energy by being heated to a temperature higher than its melting point (T_{m}), and releases it during solidification. For the determination of λ_{eff}, the steady-state comparative method was used and modified to measure composite samples at temperatures above T_{m}. Results were compared with the thermal conductivity of the pure PCMs, and a significant increase could be observed. The dependence of λ_{eff} on temperature, as well as the influence of the material microstructure on the enhancement of λ_{eff}, were examined.

Keywords Graphite · Latent thermal energy storage · Phase change materials · Thermal conductivity

1 Introduction

Composite materials are very important in many engineering areas, because they can be designed to exhibit the best characteristics of their individual constituents [1].

Paper presented at the Seventeenth European Conference on Thermophysical Properties, September 5–8, 2005, Bratislava, Slovak Republic.

K. S. do Couto Aktay (✉) · R. Tamme · H. Müller-Steinhagen
Institute of Technical Thermodynamics, German Aerospace Center (DLR),
Pfaffenwaldring 38-40, 70569 Stuttgart, Germany
e-mail: katia.aktay@ike.uni-stuttgart.de

Present Address:
K. S. do Couto Aktay
Institute of Nuclear Technology and Energy Systems, University of Stuttgart,
Pfaffenwaldring 31, 70569 Stuttgart, Germany

They are ideally suited for modern technologies that require materials with an unusual combination of properties that cannot be met by conventional single-phase materials. Their properties are termed effective properties (P_{eff}) and are defined by a linear relationship between an average of a generalized local flux (F) and an average of a generalized local or applied intensity (G) [1];

$$F \propto P_{\text{eff}} G$$

For conduction problems, F represents the average local heat flux and G denotes the average local temperature gradient. The associated effective property is the effective thermal conductivity λ_{eff}. It depends on the phase properties and microstructural information, including the phase volume fractions, orientations, sizes, shapes, and spatial distribution of the phases and their connectivity [1].

The materials investigated in this work were composites consisting of a phase change material (PCM) and expanded graphite (EG) to be employed in high-temperature latent thermal energy storage systems. These systems operate typically at temperatures between 100 °C and 400 °C. They require storage materials with a thermal conductivity preferably in the range of 5 $\text{W}\cdot\text{m}^{-1}\cdot\text{K}^{-1}$– 20 $\text{W}\cdot\text{m}^{-1}\cdot\text{K}^{-1}$, and an additionally high volumetric heat capacity to guarantee high discharging power and high storage density.

The storage principle relies on the usage of a PCM, which undergoes a phase transition, usually solid–liquid; energy is stored upon melting and released during solidification. In comparison with storage of sensible heat, the storage of latent heat has the advantage of a high storage density, due to the enthalpy of fusion, and since a phase transition occurs at almost constant temperature, the storage system can be operated within small temperature variations.

Latent thermal energy storage (LTES) finds application in solar energy heating and cooling, thermal protection of electronic devices, transport of temperature sensitive materials, building materials, etc. [2,3]. At temperatures above 100 °C, applications are mainly solar thermal power generation and utilization of waste heat [4].

Materials used as PCMs must have an appropriate melting temperature, according to the operating temperature of the storage system, and preferably a high latent heat of fusion. For high-temperature LTES, potential PCMs are mainly inorganic anhydrous salts, which have very low thermal conductivity (below 1 $\text{W}\cdot\text{m}^{-1}\cdot\text{K}^{-1}$) and consequently cannot fulfill the aforementioned requirements.

It was therefore proposed to use expanded graphite, in the form of flakes and as a porous matrix, to increase the thermal conductivity of the PCMs. The prepared PCM/graphite composites are termed composite latent storage materials (CLSM). They are expected to have their thermal conductivity basically determined by the graphite content and/or structure and the adequate melting temperature and high storage capacity of the PCM [5].

The present work reports on the measurement of the effective thermal conductivity (λ_{eff}) of such composites in a temperature range below and above the melting temperature of their PCMs. It also discusses the influence of the composite microstructure on λ_{eff}.

Table 1 PCMs used for manufacturing of composites

	PCM 1	PCM 2
Composition	68 mass% KNO_3 32 mass% $LiNO_3$	54 mass% KNO_3 46 mass% $NaNO_3$
Melting Point	133°C	222°C

Composition is given in percent by mass (mass%)

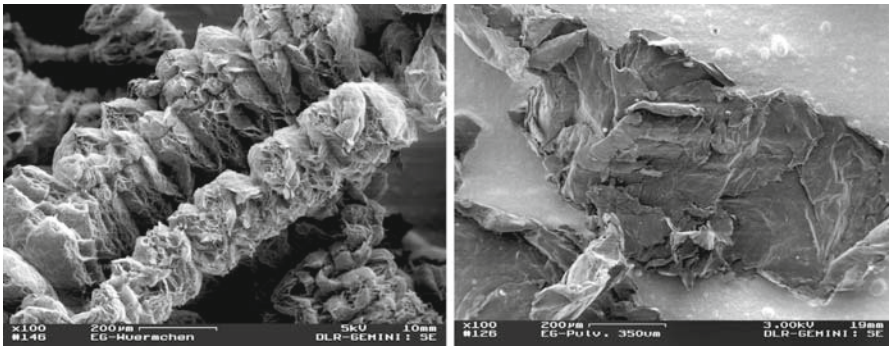

Fig. 1 Scanning electron micrographs of vermicular expanded graphite (left) and ground expanded graphite flakes (right)

2 Materials

Composites were fabricated by infiltration and compression using PCM and expanded graphite, with a PCM content of 85 % by mass. Detailed preparation of samples is given in [5].

Two alkali nitrate salt systems were employed as PCM, namely, the eutectic mixtures: potassium nitrate (KNO_3)—lithium nitrate ($LiNO_3$), and potassium nitrate—sodium nitrate ($NaNO_3$). Their composition and melting temperatures [6] are summarized in Table 1.

Expanded graphite is manufactured from graphite flakes and shows a vermicular structure as shown in Fig. 1. It has a very low bulk density and can be compacted into stable graphite sheets, without the addition of binding materials, to form highly porous graphite matrices with anisotropic thermal properties. For fabrication of compressed samples, ground expanded graphite flakes are more adequate [5]; their structure is also shown in Fig. 1.

3 Microstructure

3.1 Infiltrated Composites

Composites fabricated by infiltrating molten PCM 1 into a porous expanded graphite matrix had a content of ca. 10 %–15 % graphite by volume (vol%), 65 vol%–78 vol% PCM, and some residual porosity.

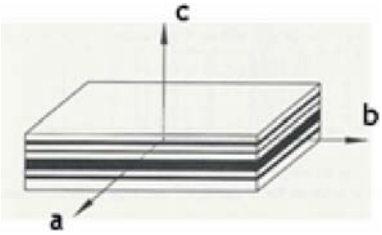

Fig. 2 Idealized laminate composite with alternating layers of phases of random thickness [1]

Owing to the layered structure of the matrix, these composites can be idealized as simple laminates and the treatment presented in [1] can be applied for predicting λ_{eff}. Laminates consist of alternating layers of phases 1 and 2, graphite and PCM, respectively, of random thickness, with volume fractions φ_1 and φ_2 and thermal conductivities $\lambda_1 \gg \lambda_2$. These composites are macroscopically anisotropic, and the effective thermal conductivities along the principal axis in the laminates, as depicted in Fig. 2, are given by

$$\lambda_{(a-b \text{ plane})} = \lambda_1\varphi_1 + \lambda_2\varphi_2,$$

the arithmetic average of the phase conductivities, and

$$\lambda_{(c\text{-axis})} = \frac{\lambda_1\lambda_2}{\lambda_1\varphi_2 + \lambda_2\varphi_1},$$

the harmonic average of the phases.

The arithmetic average corresponds to conduction along the slabs (a–b plane), where the phases are connected and the heat flow is relatively unimpeded, even if one phase is a poor conductor. The harmonic average, on the other hand, corresponds to conduction perpendicular to the slabs (c-axis) and the heat flow is relatively impeded in this direction [1].

As λ_1 is not known, the enhancement of λ_{eff} due to the addition of graphite could be estimated considering the simple laminate model and different λ_1/λ_2 ratios. Figures 3 and 4 show that laminates with φ_2 between 0.6 and 0.8 have an enhanced effective conductivity along the slabs of ca. 20 %–40 % of the graphite conductivity, and perpendicular to the slabs, less than 20 % of λ_1.

3.2 Cold Compressed Composites

These composites were fabricated by compressing PCM 2 and ground expanded graphite flakes at room temperature, consisting of ca. 80 % PCM by volume.

Figure 5 presents scanning electron micrographs which depict the distribution of the phases in the material. On the left micrograph, the material after manufacturing is shown, where the white, light grey, and dark phases represent sodium nitrate, potassium nitrate, and graphite, respectively.

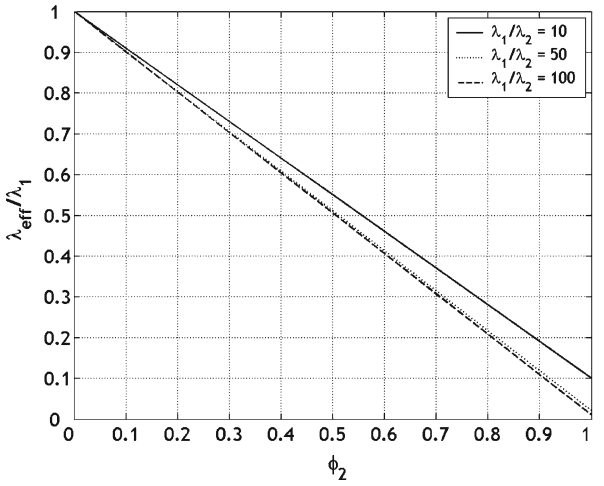

Fig. 3 Theoretical effective thermal conductivity along the slabs of a laminate for different phase thermal-conductivity ratios

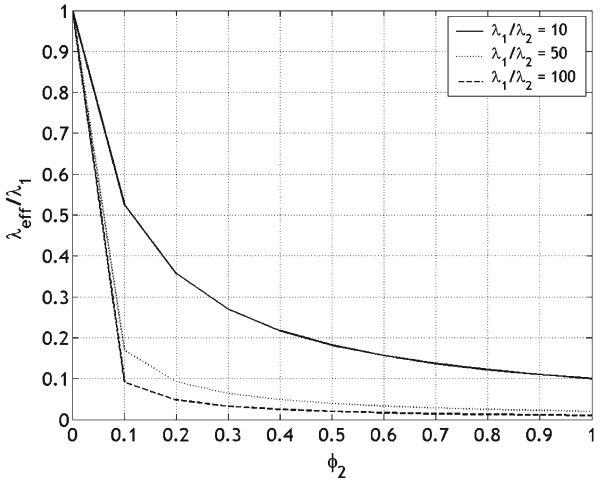

Fig. 4 Theoretical effective thermal conductivity perpendicular to the slabs of a laminate for different phase thermal-conductivity ratios

Cold compressed composites may differ from infiltrated ones in that their microstructure may be more influenced by phase change. Therefore, some samples were thermally cycled. One thermal cycle consisted of three phases: a heating phase at $10\,\mathrm{K}\cdot\mathrm{min}^{-1}$ until the melting temperature of the PCM T_m, an isothermal phase at T_m, and a cooling phase at $10\,\mathrm{K}\cdot\mathrm{min}^{-1}$ down to room temperature.

It was observed that after thermal cycling, i.e., after the composite experienced some melting/solidification cycles, potassium and sodium nitrate do not appear as separate phases (on the right micrograph). PCM and graphite are distributed differently, and the material presents some porous and solid regions. The composite has interpenetrating

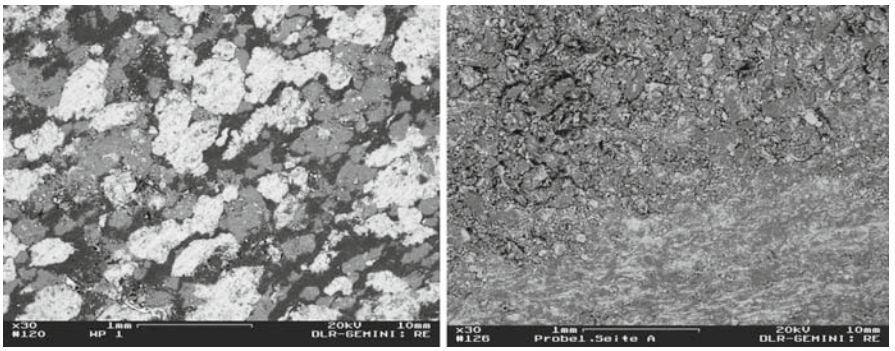

Fig. 5 Scanning electron micrographs of cold compressed samples: after fabrication (left) and after being thermally cycled (right)

phases and exhibits a significant change in microstructure. Cold compressed composites are, therefore, expected to behave macroscopically isotropic.

The aforementioned laminate model can be considered as upper and lower bounds for macroscopically isotropic composites [1]. The arithmetic average overestimates λ_{eff} and represents an upper bound, while the harmonic average underestimates λ_{eff} and is a lower bound on the effective conductivity. The enhancement due to graphite can thus be predicted to lie between the limits determined by the simple laminate model, given in Figs. 3 and 4 for different phase conductivity ratios.

3.3 Warm Compressed Composites

These composites differed from the cold compressed ones only in that the fabrication process was carried out at 180 °C. They consisted of ca. 80 % PCM 2 by volume.

The distribution of the phases in the material is depicted in Fig. 6. The left micrograph shows that the phases are distributed less homogeneously than in the cold compressed composite (left micrograph in Fig. 5). After thermal cycling (right micrograph), PCM exists as a single phase and the microstructure changes; some local porosity can be observed. It is expected that these composites have an isotropic thermal behavior as well, but λ_{eff} may be lower than for cold compressed samples due to the poorer interconnectivity of graphite in the material.

λ_{eff} can also be predicted considering the upper and lower bounds given by the laminate model in Figs. 3 and 4.

4 Measurement of Thermal Conductivity

4.1 Requirements

The measurement of the thermal conductivity of composites comprising PCM and graphite imposes some practical problems. Specimens should be measured without need for machining, so that an integral behavior of the material, including local

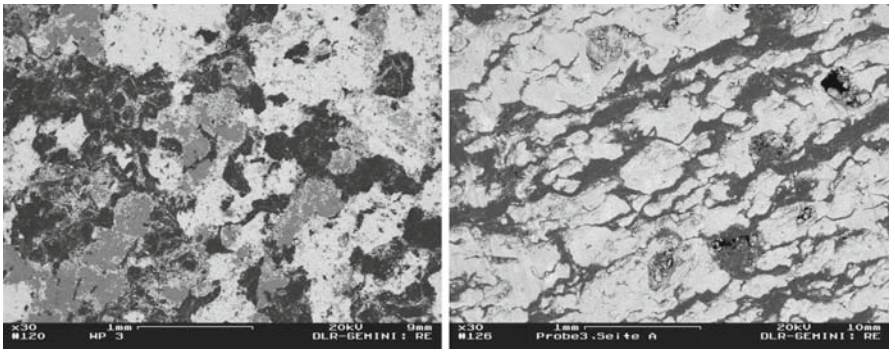

Fig. 6 Scanning electron micrographs of warm compressed samples: after fabrication (left) and after being thermally cycled (right)

volume fraction fluctuations, can be considered. For thermal storage, changes in thermal conductivity of the storage materials due to melting/solidification cycles must also be known. Regarding composites with partial phase change, their thermal behavior must be understood for the whole temperature range of operation of the storage, which can be divided into three stages with the following characteristics: (1) below the melting point T_m, where two solid phases exist; (2) at T_m, where the graphite content does not change phase and the PCM exists in solid and liquid phases, and (3) above T_m, where one solid and one liquid phase exists. In this last step, it must be also considered that the PCM may not be entirely in the liquid phase and that the transfer of heat in the composite may be good enough not to allow the entire PCM content to melt, which would result in loss of storage capacity. Furthermore, specimens do not have the same dimensions and surface characteristics, and may also have different radiative properties; some of them may become porous and others may lose structural integrity during the measurement, demanding the usage of a container.

To understand these various effects and fulfill all discussed requirements, one single method may not be sufficient and different alternatives may be used for determining λ_{eff} and evaluating the different effects on it.

4.2 Measurement Methods

Many techniques are available for measuring the thermal conductivity of solid materials. They apply either a time-dependent temperature response of the material for calculating its thermal conductivity or the measurement of the temperature difference under steady-state conditions.

Three methods were available for the present work and will be discussed briefly concerning applicability to the specimens under investigation.

4.2.1 Transient Plane Source (TPS) Technique

The TPS technique, also known as the hot disk, was described by Gustafsson [7]. It is a transient method based on an electrically isolated plane resistive element used as

the heat source and temperature sensor, which is sandwiched between two specimen halves. A constant current is applied to the specimen and the transient temperature increase in the sensor is recorded, from which both thermal conductivity and thermal diffusivity can be evaluated.

A major advantage of this technique for measuring the present composite materials over other transient methods is that specimens with different dimensions can be measured, and both the thermal conductivity and the thermal diffusivity can be evaluated simultaneously without the need of additional accurate sample properties. The use of a container for high-temperature measurements implies some practical restrictions regarding adaptability to the hot-disk setup. Measurements above the melting temperature of PCM 2 face two additional limitations: one imposed by the contact of molten salt with the high temperature mica sensor and if using Kapton sensors, the one imposed by the thermal stability of the Kapton foil.

4.2.2 Laser Flash Technique

The laser flash technique, first described by Parker et al. [8], is also a transient technique whereby the front face of a sample is heated by a short laser pulse, eliminating the problem of the thermal contact resistance. The temperature rise on the rear surface of the specimen is measured over time and used to calculate the thermal diffusivity.

The advantage of this method is the non-contact measurement principle, where no limitation due to the sensing element exists, along with the possibility of measuring our specimens above the melting temperature of the PCMs. The method has the disadvantage of requiring additional accurate data for the calculation of the thermal conductivity of the specimens. The required very small specimens represent another major limitation, because thermal cycle effects cannot be investigated with the entire composite sample.

4.2.3 Steady-State Comparative Method

The steady-state comparative method was described by Tye [9] and uses the comparison of parameters of an unknown specimen with those of materials of known properties. It basically consists of a specimen joined directly to one reference material or sandwiched between two reference materials and surrounded by a guard cylinder. A temperature gradient is established along the test stack, and longitudinal heat flow is assured or maximized by adjustment of either the temperature gradient in, or the isothermal temperature of, the guard cylinder.

Concerning the present composites, this method has the advantage of being adaptable to the different specimen dimensions and shapes. Furthermore, with appropriate container composites, this technique can be used for measurements above T_{m}. The main disadvantages are the interfacial thermal resistance between reference samples and composite specimens with different surface finishing, the long measurement time, and lower accuracy in comparison with more sophisticated methods.

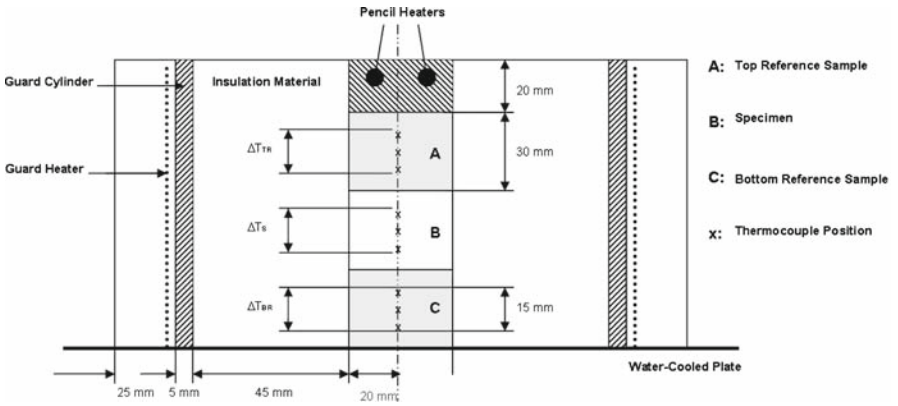

Fig. 7 Schematic of the comparative apparatus

5 Experimental Apparatus

The steady-state comparative method was chosen for the determination of λ_{eff} of the composite materials. For the purpose of this study, the method allows measurements with available sample dimensions, and composites can be measured above the melting temperature with suitable modifications. As materials do not need to be machined for the measurement, it is possible to cycle the samples in an external oven and repeat the measurement. The advantage of a simple mathematical evaluation of results avoids additional uncertainties of other, not well-known properties of the composites. To fulfill the previously mentioned requirements, a compromise must be found between the acceptable accuracy that can be reached with the materials studied and the practical attempts. Taking all this into account, the comparative method seems to be the most adequate for an initial understanding of the transfer of heat in PCM/graphite composites.

The designed apparatus consisted of a stack of cylindrical samples, as depicted schematically in Fig 7. The specimen of unknown thermal conductivity was placed between two similar samples of reference material. Above the upper reference sample, heat was generated in pencil heaters fitted in a copper sample. The bottom reference sample was placed on a water-cooled cold plate. The sample stack was surrounded by fiber glass insulating material, 45 mm thick, and with a thermal conductivity λ_{I} of $0.034\ \text{W}\cdot\text{m}^{-1}\cdot K^{-1}$ and $0.042\,\text{W}\cdot\text{m}^{-1}\cdot\text{K}^{-1}$ at 20 °C and 100 °C, respectively. The entire assembly was enclosed within a cylindrical metal guard heated by a three-zone controlled heater.

Considering the wide range of thermal conductivities, from less than $1\,\text{W}\cdot\text{m}^{-1}\cdot\text{K}^{-1}$ for the pure PCMs to $30\,\text{W}\cdot\text{m}^{-1}\cdot\text{K}^{-1}$ in the radial direction for the porous graphite matrix, stainless steel AISI321 (DIN 1.4541), with a thermal conductivity λ_{R} around $15\,\text{W}\cdot\text{m}^{-1}\cdot\text{K}^{-1}$ (at room temperature), was chosen as a suitable reference material. λ_{R} was obtained from data published by Perovič et al. [10] and is plotted as a function of temperature in Fig. 8. Specimens were 40 mm in diameter with the length varying

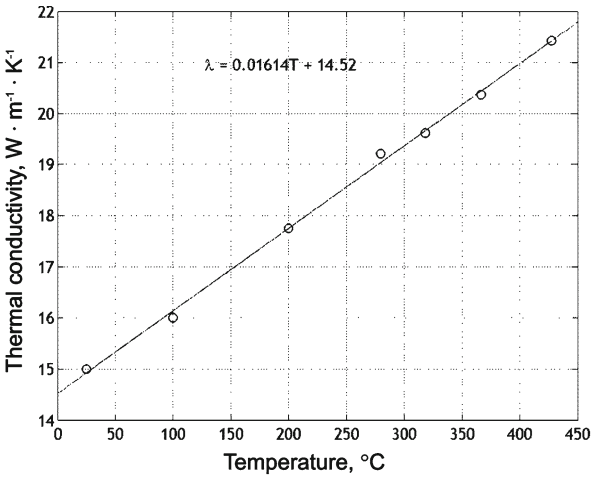

Fig. 8 Thermal conductivity of reference material AISI 321 [10]

between 10 mm and 20 mm; therefore, the top and bottom reference samples were 30 mm long.

The temperature was measured by fine gauge metal-sheathed chromel/alumel thermocouples with an overall diameter of 0.25 mm and read out using an Agilent 34970A digital multimeter. In both the reference samples and the specimen, three thermocouples were placed at equidistant positions. They were fitted tightly into small holes, 0.30 mm in diameter and 3 mm deep, drilled longitudinally in the materials.

For the evaluation of λ_{eff}, a steady-state condition was reached for a temperature drift rate smaller than the thermocouple uncertainty. λ_{eff} was calculated considering the temperature differences measured in the stack and an average apparent heat flux was calculated as

$$\lambda_{\text{eff}} = \left[\frac{1}{2}\left(\lambda_{\text{TR}}\frac{\Delta T_{\text{TR}}}{\Delta L_{\text{TR}}} + \lambda_{\text{BR}}\frac{\Delta T_{\text{BR}}}{\Delta L_{\text{BR}}}\right)\right]\frac{\Delta L_{\text{S}}}{\Delta T_{\text{S}}}$$

where ΔT and ΔL are the temperature difference and the distance between thermocouples, respectively. The subscripts TR, BR, and S stand for top reference sample, bottom reference sample, and composite specimen, respectively. λ_{eff} was evaluated for all specimens in the direction parallel to the heat flux imposed to the sample stack.

For measurements at higher temperatures, the apparatus was modified following the test cell idea reported by Tye et al. [11]. A reference sample was fabricated from stainless steel AISI321 with a cavity to be used to contain the specimen. The dimensions of the reference sample were 44 mm in diameter and 40 mm in height, including the cavity of 42 mm in diameter and 10 mm high. Thermocouples were placed at equidistant positions in the wall of the cavity and in equidistant holes along the reference material.

The uncertainty of the method relies basically on the thermal conductivity of the reference materials and the temperature measurement. In order to check the apparatus,

Table 2 Composites measured with the comparative apparatus

Composite No.	Phase change material	Fabrication process	Thermal cycling[a]	Specimen length (mm)
1	PCM 1	Infiltration	–	10
2	PCM 2	Cold compression	–	20
3	PCM 2	Cold compression	6	10
4	PCM 2	Warm compression	–	10
5	PCM 2	Warm compression	2	10

[a] Refers to number of thermal cycles

a graphite specimen, previously measured with the method standardized in the norm DIN 51908, was tested. This norm defines a steady-state comparative method for testing of carbon materials at room temperature.

6 Results and Discussion

Measurements with the described apparatus were made at successive increasing temperatures, from room temperature to about 50 °C above the melting point.

Measurements showed that an isothermal guard heater with a temperature slightly above the specimen temperature enabled measurements with small deviations. The deviation between apparent heat fluxes was kept below 20 %. The graphite sample used for testing the apparatus showed a deviation of 12 % from the value previously measured with the method described in the norm DIN 51908. Measured specimens are summarized in Table 2.

Experimental results are presented in Figs. 9 and 10, where λ_{eff} is plotted as a function of temperature. The values of the thermal conductivity of the pure alkali nitrates used for comparison were from the literature. The thermal conductivity of lithium nitrate, sodium nitrate, and potassium nitrate in the solid phase are published in Tye et al. [11], Yoshida and Sawada [12], White and Davis [13], respectively. Data for all nitrates above the melting point are from McDonald and Davis [14]. The dashed line represents the melting point of the PCM.

Composite 1, consisting of PCM 1 infiltrated in the porous expanded graphite matrix, was measured perpendicular to its layers. Owing to its anisotropy, the measured effective thermal conductivity corresponds to the axial effective thermal conductivity of the material. For comparison, the thermal conductivity of PCM 1 ($\lambda_{\text{PCM 1}}$) was considered to be about $1\,\text{W}\cdot\text{m}^{-1}\cdot\text{K}^{-1}$ in the temperature range $T_{\text{m}} \pm 50\,^{\circ}\text{C}$ (approximate operating temperature of a latent thermal storage unit).

Results show that λ_{eff} of Composite 1 is approximately five times higher than $\lambda_{\text{PCM 1}}$. Below T_{m}, λ_{eff} is stable with temperature. In this temperature range, the PCM was in the solid phase and λ_{eff} seems to not be influenced by changes in $\lambda_{\text{PCM 1}}$ with temperature. Above T_{m}, PCM was in the liquid phase and λ_{eff} showed a decrease of about 11%. It may be attributed to the decrease in $\lambda_{\text{PCM 1}}$, showing the influence of liquid PCM on λ_{eff}. Both pure lithium nitrate and sodium nitrate show a significant decrease in their thermal conductivity after melting at 265 °C and 337 °C, respectively.

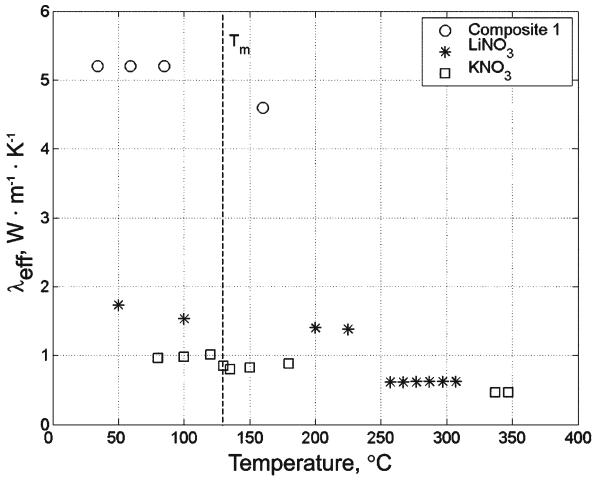

Fig. 9 Axial effective thermal conductivity of the composite material consisting of PCM 1 versus temperature. Thermal conductivities of pure lithium nitrate and potassium nitrate are included for comparison. Melting point of PCM 1 (133 °C) is represented by dashed line

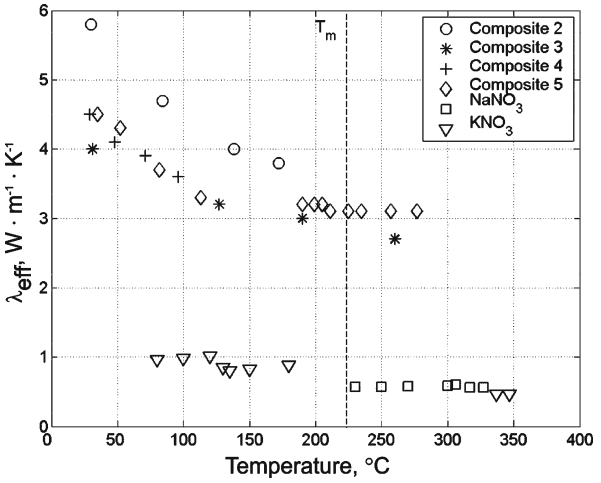

Fig. 10 Effective thermal conductivity of composites consisting of PCM 2 versus temperature (for comparison, the thermal conductivity of pure sodium nitrate and potassium nitrate are shown). Melting point of PCM 2 (222 °C) is represented by dashed line

Assuming a phase conductivity ratio λ_1/λ_2 of 50, λ_{eff} represents about 10 % of the thermal conductivity of the more conductive graphite phase. Comparing with predictions using the idealized simple laminate model, our experimental results lie near the estimated lower bound (Fig. 11). This suggests that infiltrated composites have a somewhat layered structure and that their axial effective conductive is strongly influenced by λ_{PCM}.

Measurements on Composites 2 and 4 were made only at temperatures below T_{m}. The samples had a microstructure similar to that depicted previously in the left micrographs in Figs. 5 and 6, i.e., they represent the composites after manufacturing. Before measurement, Composites 3 and 5 were thermally cycled six and two

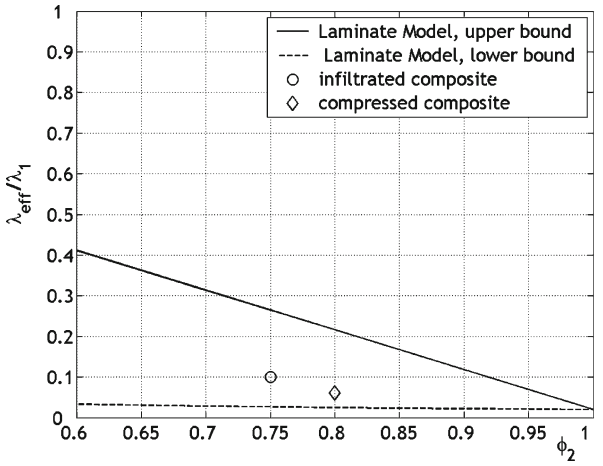

Fig. 11 Comparison between results and upper and lower bounds assuming $\lambda_1/\lambda_2 = 50$

times, respectively. Their microstructure was similar to those depicted in the right micrographs in Figs. 5 and 6. The thermal conductivity of PCM 2 ($\lambda_{PCM\,2}$) was considered for comparison between $0.5\,W\cdot m^{-1}\cdot K^{-1}$ and $1\,W\cdot m^{-1}\cdot K^{-1}$ for the relevant temperature range around T_m.

Results show that λ_{eff} of composites is significantly higher than $\lambda_{PCM\,2}$, decreasing with increasing temperature.

Comparing results for Composites 2 and 4, which did not experience any thermal cycling, they differ by up to 20 %. This may be attributed to a more homogeneous distribution of the PCM and graphite phases in Composite 2.

Results for Composite 3 show a decrease of about 30 % compared to Composite 2. This indicates that the influence of $\lambda_{PCM\,2}$ on λ_{eff} may increase due to the significant change in the microstructure of these materials after thermal cycling.

Results for Composite 5 show that λ_{eff} decreases continuously and remains stable around T_m. Below T_m, results are similar to that of Composite 4. This gives evidence on the more stable microstructure of warm compressed composites.

Results for the thermally cycled materials, Composites 3 and 5, differ slightly and are approximately $3\,W\cdot m^{-1}\cdot K^{-1}$, more than three times higher than $\lambda_{PCM\,2}$. The expected lower λ_{eff} of cycled warm compressed composites could not be confirmed.

For all composites, λ_{eff} has its higher values at room temperature. Consequently, if these values are used for design purposes, λ_{eff} is overestimated. This confirms the importance of measurements at temperatures above T_m.

Assuming λ_1/λ_2 of 50, $\lambda_{PCM\,2}$ of $1\,W\cdot m^{-1}\cdot K^{-1}$, and λ_{eff} of $3\,W\cdot m^{-1}\cdot K^{-1}$ for the compressed composites at the temperature range around T_m, λ_{eff} represents 6 % of λ_1. This result lies near the predicted lower bound given by the simple laminate model (Fig. 11). It indicates that compressed composites have their λ_{eff} determined by the low thermal conductivity of the PCMs. A limited improvement can be reached if no stable graphite network exists in the material.

7 Conclusions and Outlook

In this work, composites based on a phase change material (PCM) and expanded graphite (EG) were investigated regarding their effective thermal conductivity. These composites were manufactured either by infiltrating the molten PCM into a highly porous expanded graphite matrix or by compacting a mixture of PCM and expanded graphite flakes. Infiltrated and compressed composites presented different microstructures as a result of the layered structure of the graphite matrix and of the random distribution of the PCM and graphite phases, respectively. Composite samples were measured with an apparatus based on the comparative method, built to fulfill specific requirements of the materials. Results showed a considerable improvement of the thermal conductivity. It was observed that changes in the microstructure of the materials due to thermal cycling have influence on their thermal properties.

The results of the presented study permit us to draw the following conclusions:

(a) Infiltrated composites are less influenced by changes in the properties of the PCM, and seem to have an effective thermal conductivity based on the bulk thermal conductivity of the graphite matrix.
(b) Manufacturing parameters for preparation of compressed composites are decisive for the distribution of the phases, interconnectivity of graphite, and formation of stable materials.
(c) Compressed composites are dynamic materials; they experience changes in their microstructure because of melting/solidification cycles, which influence their thermal conductivity. Such effects must be studied in detail for a correct understanding of the changes in the properties of PCM/graphite composites.
(d) The effective thermal conductivity of PCM/graphite composites must be studied over the temperature range relevant for their application.

Current research activities focus on the measurement of the radial effective thermal conductivity of the composites. These data will enable better characterization of the anisotropic behavior of infiltrated composites and give more insight into compressed composites.

Further investigations using the laser-flash technique are planned and may give additional information about transient effects in the composites. The shorter measurement times may also allow more samples to be studied. The lack of data about the thermal conductivity of the binary alkali nitrate systems also motivates their measurement.

Acknowledgments We are thankful to the Bavarian Center for Applied Energy Research (ZAE Würzburg) for the measurement of the thermal conductivity of the fiber glass insulation material. We also thank SGL Technologies for supplying graphite samples.

References

1. S. Torquato, *Random Heterogeneous Materials—Microstructure and Macroscopic Properties* (Springer-Verlag, New-York, 2002)
2. B. Zalba, J. Marín, L.F. Cabeza, H. Mehling, Appl. Therm. Eng. **23,** 251 (2003)
3. M.M. Farid, A.M. Khudhair, S.A.K. Razack, S. Al-Hallaj, Energy Convers. Manage. **45**, 1597 (2004)

4. R. Tamme, W.-D. Steinmann, D. Laing, in *Proceedings of the 9th International Conference on Thermal Energy Storage—Futurestock 2003* (Warsaw, 2003), pp. 191–199
5. K.S. do Couto Aktay, R. Tamme, H. Müller-Steinhagen, in *Proceedings of the 2nd Phase Change Material and Slurry Conference* (Yverdon-les-Bains, 2005), pp. 89–97
6. G.J. Janz (ed.), *NSRDS-NBS* **61**, Part II (1979)
7. S.E. Gustavsson, Rev. Sci. Instrum. **62**, 797 (1991)
8. W.J. Parker, R.J. Jenkins, C.P. Butler, G.L. Abbott, J. Appl. Phys. **32**, 1679 (1961)
9. R.P. Tye, in *Compendium of Thermophysical Property Measurement Methods*, ed. by K.D. Maglić, A. Cezairliyan, V.E. Peletsky, Vol. 1 (Kluwer Academic/Plenum Publishers, New York, 1992), pp. 77–97
10. N.L. Perovič, K.D. Maglić, A.M. Stanimirović, G.S. Vuković, High Temp. High Press. **27/28**, 53 (1995/1996)
11. R.P. Tye, A.O. Desjarlais, J.G. Bourne, in *Proceedings of the 7th Symposium on Thermophysical Properties* (ASME, 1977), pp. 189–197
12. I. Yoshida, S. Sawada, J. Phys. Soc. Jpn. **15**, 199 (1960)
13. L.R. White, H.T. Davis, J. Chem. Phys. **47**, 5433 (1967)
14. J. McDonald, H.T. Davis, J. Phys. Chem. **74**, 725 (1970)